



This document is a postprint version of an article published in Journal for Nature Conservation© Elsevier after peer review. To access the final edited and published work see <https://doi.org/10.1016/j.jnc.2022.126221>

Document downloaded from:



1

2 **Point pattern analysis as a tool for assessing disease**

3 **spread and population features in remaining sanctuaries**

4 **of the critically endangered bivalve *Pinna nobilis***

5 Patricia Prado<sup>1,2\*</sup>, Miguel Ángel López<sup>3</sup>, Pablo Cermeño<sup>4</sup>, Ferrán Bertomeu<sup>5</sup>, Jose Rafael García-  
6 March<sup>2</sup>, Sebastián Hernandis<sup>2</sup>, José Tena-Medialdea<sup>2</sup>, Emilio Cortés<sup>6</sup>, Francisca Giménez-  
7 Casalduero<sup>7</sup>

8

9 Running title: Population condition in *Pinna nobilis*

10

11 <sup>\*1</sup>IRTA-Sant Carles de la Ràpita. Ctra. Poble Nou Km 5.5, 43540 Sant Carles de la Ràpita,  
12 Tarragona, Spain

13 <sup>2</sup>Institute of Environment and Marine Science Research (IMEDMAR-UCV), Universidad Católica  
14 de Valencia SVM, C/Explanada del Puerto S/n, 03710 Calpe, Alicante, Spain

15 <sup>3</sup>Forestal Catalana, Ministry of Climate Action, Food and Rural Agenda, Generalitat de  
16 Catalunya. C/ Torrent de l'Olla, 218, 08012 Barcelona, Spain

17 <sup>4</sup>Fundació Zoo de Barcelona, Parc de la Ciutadella, 08003 Barcelona

18 <sup>5</sup>Institute of Environmental Science and Technology (ICTA), Autonomous University of  
19 Barcelona. Carrer de les Columnes s/n, UAB Campus, 08193 Cerdanyola del Vallès, Barcelona

20 <sup>6</sup>Acuario de la Universidad de Murcia, Cuartel de Artillería, C/ Cartagena s/n. 30002 Murcia

21 <sup>7</sup>Department of Marine Science and Applied biology, University of Alicante, Carretera de Sant  
22 Vicent del Raspeig s/n, 03690 San Vicente del Raspeig, Alicante, Spain

23 ABSTRACT

24 An emergent disease has relegated populations of the Mediterranean pen shell, *Pinna nobilis*  
25 L. critically endangered to sanctuaries featuring salinities outside the 36.5 to 39 range. Point  
26 pattern analysis was used in three areas of the Alfacs Bay (Ebro Delta) still hosting pen shells to  
27 assess the possible undergoing of disease spread by comparing the spatial distribution of live  
28 individuals vs. empty shells across spatial scales. We also evaluated the importance of other  
29 ecological aspects of conservation relevance such as the size distribution of individuals, and  
30 the possible association to seagrass habitats. The population assessment showed no recent  
31 mortality and a clear dominance of large adults among empty shells (97.3%) pointing to no  
32 disease spread during the study period. At the low spatial scale Nearest Neighbor (NN)  
33 analyses evidenced significant clustering (NN Ratios of 0.4-0.8), but in one of the zones NN  
34 distances were closer in empty shells than in live individuals, suggesting a former localized  
35 outbreak. At the larger spatial scale, MDSCA confirmed clustering patterns up to distances of  
36 115 to 190 m, with higher aggregation of empty shells at the same study zone. The bay also  
37 featured low juvenile availability (3.2%), which risks the continuity of the population. No  
38 evidence for habitat or conspecific selection could be observed from abundance patterns and  
39 variation in NN across study regions. Our research provides a tool for assessing population  
40 condition in paralic environments, where salinity conditions tend to slow down disease spread,  
41 thus allowing a time gap for undertaking conservation decisions.

42

43 *Keywords:* spatial distribution; Nearest Neighbor Analysis; Multi-distance Spatial Cluster  
44 Analysis; size class structure; population condition

## 45 1. Introduction

46 The fan mussel, *Pinna nobilis*, is an endemic Mediterranean bivalve currently listed as a  
47 “critically endangered” species by the Spanish government (BOE 251–14181, 2018), and the  
48 International Union for Conservation of Nature (IUCN) (Kersting et al., 2019). In the fall of  
49 2016, mass mortality events (MMEs) close to 100% of the individuals started to occur in  
50 southern Spanish waters and have spread to the rest of the Mediterranean Sea in less than  
51 three years (García-March et al., 2020b). The etiological agent responsible for MMEs was first  
52 identified as the protozoan *Haplosporidium pinnae* (Catanese et al., 2018), although synergistic  
53 effects with a new species of *Mycobacterium* (Carella et al., 2019; 2020; Šarić et al., 2020)  
54 and/or Vibriosis (Rodríguez et al., 2018, Prado et al., 2020b, Künili et al., 2021; Lattos et al.,  
55 2021) cannot be discarded. At present, only isolated populations in reservoirs such as coastal  
56 bays and lagoons featuring salinity conditions frequently outside the 36.5 to 39 range appear  
57 to experience lower shellfish mortality rates associated to the disease (e.g., Cabanellas-  
58 Reboredo et al., 2019; Prado et al., 2021; Katsanevakis et al., 2021) and may act as larval  
59 sources for a future recovery of the species. However, due to their semi-closed regimes, these  
60 areas are subjected to large environmental variations, which may bring them close to the  
61 optimum conditions for the disease. Having a tool to detect the spread of mortalities and  
62 simultaneously assess local population dynamics, is fundamental for the long-term  
63 conservation of populations.

64 The spatial arrangement of benthonic communities is decided in the moment of settlement  
65 and metamorphosis as well as by benthic processes occurring at local spatial scales (Prado et  
66 al., 2012). Gregarious settlement usually occurs in response to an attractive substance or  
67 stimuli that is associated with the presence of a suitable habitat or conspecifics (Woodin 1986;  
68 Kingsford et al., 2002). Further patterns of aggregation may also arise from rejection of some  
69 types of discrete substrates because of the presence of negative cues including surface texture  
70 and conspecifics pheromones as observed for the barnacle *Balanus improvisus* (Berntsson et

71 al., 2004). Larval settlement may be also affected by passive factors such as depth (Prado et al.,  
72 2020a) since shallow areas constitute a physical barrier that can alter the direction or speed of  
73 currents. Spatial patterns of populations are expected to reflect larval settlement selection and  
74 a combination of passive transport patterns and larval planktonic behavior (Hoffmann et al.,  
75 2012). Such patterns may be obscured by early benthic processes such as physical disturbance,  
76 predation, and competition and/or physiological stress and disease which may cause large  
77 mortalities of over 90% of all juveniles (Hunt & Scheibling, 1997; Gosselin & Qian, 1997). Yet,  
78 mapping and imaging techniques are still considered to provide a valuable 'footprint' of factors  
79 determining settlement patterns in sessile organisms (Gosselin & Qian, 1997).

80 Spatial pattern analysis is a widely used technique in the field of forest ecology to  
81 understand propagule dispersal and vegetative reproduction processes that characterize the  
82 life strategy and colonization success of plant species (Hamill and Wright, 1986; Little and Dale,  
83 1999). It has been successfully used to assess the effects of intra- and interspecific  
84 competition, the spread of contagious diseases, or growth facilitation by other species in wild  
85 vegetal populations (Kenkel, 1988; He & Duncan, 2000; Rejmánek & Lepš, 1996; Haase et al.,  
86 1996; Moeur, 1997; Gienke et al., 2014; Maggi et al., 2017). For instance, Kenkel (1988)  
87 examined the positions of live and dead trees and found that the distribution of live trees was  
88 locally highly regular indicative of an inhibition distance, while the dead trees were  
89 significantly more clumped than random mortality would dictate. Haase et al., (1996) observed  
90 significantly clumped patterns resulting from a strong association with other persistent plant  
91 species whereas seedlings germinating under the canopy of conspecifics tended to die within  
92 days or weeks. Among distance-based methods, the cumulative distribution function given by  
93 the distance to the nearest neighbor (Clark & Evans, 1954) and the Ripley's  $K$  function (Ripley,  
94 1977) are two of the most widely used approaches for mapped data (see reviews by Liu, 2001;  
95 Dixon, 2002). The nearest neighbor analysis is useful for assessing processes occurring at the  
96 small spatial scale but does not allow detecting distances between aggregates whereas the  $K$

97 function allows for the analysis of patterns at a hierarchy of scales, including the distances  
98 between aggregates, since it is based on the distances between each point and all the other  
99 points in the pattern (Rozas & Camarero, 2005). Potentially, these tools could be also applied  
100 to study the spatial arrangement of sessile marine invertebrates after pelagic dispersion from  
101 adult sources as well as for detecting possible infection outbreaks by comparing aggregation  
102 patterns of living versus dead individuals. However, to our knowledge, this is a disregarded  
103 approach in the marine environment, possibly because it is not always possible to obtain a  
104 point map of the target species distribution and alternative methods such as quadrates and  
105 transects have prevailed (e.g., Basso et al., 2015; Cox et al., 2017).

106 Spatial patterns of distribution may be more easily obtained for large sessile species such as  
107 *Pinna nobilis* thus providing valuable information about the possible influence habitat features  
108 and/or the presence of conspecifics in spatial patterns of distribution. Pen shell MMEs are  
109 caused by a disease that appears to be very highly specific and infective in open waters  
110 (García-March et al., 2020b). However, infection rates can be considerably decreased in paralic  
111 environments with salinities outside the 36.5 to 39 range, particularly in non-summer periods  
112 (Prado et al., 2021) and are therefore expected to reflect foci of infection and the potential  
113 spread of the pathogen(s) when comparing point patterns of live individuals vs. empty shells.  
114 Other monitoring techniques such as PCR are so far of limited efficiency because unequivocal  
115 diagnosis requires the sacrifice of the animal for a biopsy of the digestive gland (Mihaljević et  
116 al., 2021), and post-mortem evaluation is also complicated by rapid decomposition of tissues  
117 in seawater (Brooks 2016, Huang et al., 2021). Besides, this technique alone also fails in  
118 providing spatial patterns of disease spread, which is highly necessary for decision makers  
119 prior to the implementation of possible conservation actions such as localized translocation of  
120 remaining animals, or freshwater treatments to maintain salinities below the 36.5 threshold  
121 (Cabanellas-Reboredo et al., 2018; Prado et al., 2021).

122 In this context, three different areas of the Alfacs Bay still featuring important numbers of  
123 individuals were evaluated with the following objectives: (1) to assess the occurrence of  
124 possible disease outbreaks by comparing patterns of spatial distribution in live individuals vs.  
125 empty shells in terms of density and dispersion (i.e., regular, random or clumped) across  
126 spatial scales ranging from 10s to 100s of m using spatial analysis techniques of point patterns;  
127 (2) to evaluate the size distribution of individuals (juveniles, young adults, and adults) as a  
128 proxy of the frequency of recruitment events needed for the persistence of the species, and  
129 estimate age-dependent mortality; and (3) to assess abundance patterns by habitat type and  
130 depth in order to identify possible habitats of conservation interest. In addition, we provide an  
131 updated evaluation of the status of remaining populations of *P. nobilis* in different areas of the  
132 Alfacs Bay, one of the last sanctuaries of species in the Western Mediterranean.

133

## 134 **2. Materials and Methods**

### 135 *2.1. Study areas*

136 Alfacs Bay is a semi-enclosed estuarine water body with an approximate surface of 49 km<sup>2</sup>  
137 and a maximum depth of ca. 6 m. It is located in the southern part of the Ebro River Delta  
138 (Catalonia, NW Mediterranean), and has a great economic importance due to the presence of  
139 extensive shellfish aquaculture, particularly racks of Pacific oyster and Mediterranean mussel  
140 along its northern coast. The study was conducted in three zones of the bay that still host  
141 populations of *Pinna nobilis* (Prado et al., 2020a; Prado et al., 2021): i) Zone 1 is in the middle  
142 region of the Banyà Peninsula; ii) Zone 2 in the far end of the Trabucador sand bar; and iii)  
143 Zone 3 is in the north coast of the Alfacs Bay, adjacent to the St. Joan Tower (Fig. 1).

144 Zones 1 and 2 are located within the Natura 2000 network area, with pen shell individuals  
145 distributed along the shallow sandbar (ca. 0 to 130 cm depth) that constitute the ancient  
146 coastline of the delta and features meadows of the seagrass *Cymodocea nodosa* (Ucria) Asch.,  
147 and/or beds the green macroalgae *Caulerpa prolifera* (Forsskål) J.V.Lamouroux, 1809 on a sand

148 bed (Prado et al., 2014). The pen shell parasite *H. pinnae* was detected in few individuals in  
149 Zone 1 in 2018 and 2020, whereas *Mycobacteria* sp. seems to be absent in middle and inner  
150 regions of the Bay (Prado et al., 2021). However, no previous information on pathogen's  
151 presence is specifically available for Zones 2 and 3. No MMEs have been reported in these  
152 zones, and the occurrence of the parasite is expected to decrease closer to the Trabucador  
153 Sand Bar due to slightly lower salinities (Prado et al., 2021). Zone 3 is located immediately in  
154 front of rice field drainage channels that seasonally release freshwater high in nutrients and  
155 organic matter that favors the development of epiphytes and fast growing macroalgae (Prado,  
156 2018) but also causes the reduction in salinity that appears to be protecting pen shells from  
157 MMEs (Prado et al., 2021). During preliminary surveys conducted in summer 2020, no  
158 evidence of disease was observed in this region of the bay (P. Prado, personal observation).  
159 The area hosts *Zostera noltei* in shallow silty and muddy areas closer to the freshwater  
160 discharge, while deeper areas (up to ca. 200 cm) are fully dominated by *C. prolifera* with some  
161 patches of *C. nodosa* (Prado, 2018).

162

## 163 2.2. Field sampling

164 Measures of salinity and temperature were conducted weekly in the different study zones  
165 using a YSI 6660 multiparametric probe equipped with a 650 MDS data logger in order to  
166 capture as much as possible temporal variability in these variables that could influence disease  
167 outbreaks. A total of 4.1 ha were sampled in Zone 1 (Banya Peninsula), 5.8 ha in Zone 2  
168 (Trabucador), and 4.2 ha in Zone 3 (St. Joan Tower), depending on local working conditions and  
169 available human resources to conduct the search. In zones 1 and 2, water transparency and  
170 shallow depth allowed for a direct visual identification of pen shells and recorded features by  
171 observers across previously marked areas. Sampling in these two zones was usually conducted  
172 parallel to the line of the shallow sandbar. In zone 3, featuring greater depth and lower  
173 visibility conditions in most of the area, the work was conducted with the support of a snorkel



174 team that placed a position mark next to each individual for later georeferencing. Monthly  
175 salinity values were measured during the study period at each zone.

176 Pen shells were georeferenced from March to early July 2021 (a 4-month sampling period  
177 was used because previous local research has shown that mortality in the Alfacs Bay is driven  
178 by salinity patterns and not by differences in sea temperature; Prado et al., 2021) using a Leica  
179 Zeno FLX100 Smart Antenna attached to a 2-m carbon fiber pole that allowed marking a  
180 position in shallow water. The antenna was also connected to a Leica Zeno Tab 2 Rugged  
181 Android Tablet featuring the Leica Zeno Connect application for the transmission of high  
182 precision (2 cm) GNSS positions from the antenna. For each pen shell encountered, we marked  
183 the condition (live individuals or empty shells), noting also recent mortality that can be  
184 determined by the absence of fouling in the inner part of the shell. Since the Alfacs Bay is a low  
185 hydrodynamics area, empty shells may remain in their position for many years and provide  
186 knowledge about historic patterns of abundance, as well as information on mortality resulting  
187 from recent contagious diseases.

188 Animals were measured in width and their total length estimated based on a previously  
189 established relationship for the local population ( $y = 0.207x + 7.16$ ;  $R^2 = 0.718$ ;  $p < 0.0001$ ).  
190 Resulting estimates were grouped into three classes to determine size structure: i) The  
191 smallest class consisted of large juveniles of ca.  $20 \leq x < 30$  cm; ii) medium class, young adults of  
192 intermediate size ( $30 \leq x < 50$  cm), and iii) large adults  $\geq 50$  cm, which in the Alfacs Bay may  
193 attain maximum ages of ca. 7-9 years (Prado et al., 2020a). Also, depth and habitat type  
194 including seagrass meadow (*C. nodosa* and *Z. noltei*), turf of macroalgae (*C. prolifera*) or mixed  
195 beds and sandy areas were recorded. Data were downloaded into a laptop for further data  
196 analyses with different GIS software, depending on specific needs (see below).

197

198 *2.3. Data analyses*

199 The totality of the surface covered in each zone (each one with different dimensions and  
200 shape) was first split into equal units of 1,000 m<sup>2</sup>, using the divide/ modify feature into  
201 proportional parts tool available in ArcGIS Pro 10.7.1. This yielded a total of 41 units in Zone 1,  
202 58 units in Zone 2, and 42 units in Zone 3. For each zone and unit, we calculated the number of  
203 live, empty shells, and total individuals of each size, as well the number of individuals of each  
204 condition within each habitat using the count point features within polygon features tool in  
205 QGIS Desktop 3.18.2.

206 Differences in the number of individuals by size class (juveniles, young adults, and adults)  
207 among study zones was investigated with separate one-way MANOVAs for live individuals,  
208 empty shells, and total counts. Further one-way MANOVAs were also used to assess zone  
209 differences in the number of individuals within habitats (seagrass, *Caulerpa*, mixed vegetation,  
210 and sand) for each condition and total shells. Differences among zones in the number of live  
211 individuals, empty shells, and total shells were also investigated with one-way ANOVA.

212 For all MANOVAs and ANOVAs, normality (Chi-square test) and homogeneity of variances  
213 (Cochran's test) were tested, and when necessary, data were log transformed to meet these  
214 assumptions. All analyses were performed using Statistica v.12 software.

215

#### 216 *2.4. Spatial analysis techniques of point patterns*

217 The average nearest neighbor (ANN) and Multi-distance Spatial Cluster Analyses (MDSCA)  
218 available in ArcGIS 10.7.1 were used to investigate the type of point pattern distribution  
219 (random, clumped, or regular) of live individuals, empty shells, and total shells at each study  
220 area and to assess the size of potential clumps. The ANN has been proposed to be more  
221 adequate at the low spatial scale (< 20 m; Rozas & Camarero, 2005), whereas MDSCA provides  
222 more informative results at greater distances (up to 100s of m).

223 The ANN is given as the ratio between the observed mean distance between each feature  
 224 and its nearest neighbor ( $\bar{D}_o$ ) and the expected mean distance for features given in a random  
 225 pattern ( $\bar{D}_e$ ):

$$226 \quad ANN = \frac{\bar{D}_o}{\bar{D}_e} = \frac{\sum_{i=1}^n d_i/n}{0.5 \sqrt{n/A}} \quad (1)$$

227 where  $d_i$  is the distance between the feature point  $i$  and its nearest neighboring feature,  $n$   
 228 corresponds to the total number of features, and  $A$  is the total surveyed area specified by the  
 229 user and the polygon feature.

230 The average nearest neighbor z-score value for the statistic level ( $p$  value) at which  
 231 observed pattern deviated from expected random pattern was calculated as:

$$232 \quad z = \frac{\bar{D}_o - \bar{D}_e}{SE} \quad (2)$$

233 Where:

$$234 \quad SE = \frac{0.26136}{\sqrt{n^2/A}} \quad (3)$$

235

236 MDSCA in ArcGIS is a transformation of the original Ripley's  $K$  Function which is named as  
 237  $L(d)$ :

$$238 \quad L(d) = \sqrt{\frac{A \sum_{i=1}^n \sum_{j=1, j \neq i}^n K_{i,j}}{\pi n (n-1)}} \quad (4)$$

239 where  $d$  is the distance,  $n$  is the total number of point features in the study area feature ( $A$ ),  
 240 and  $K_{i,j}$  is a weight. Depth was used as a weight field in the model in order to account for  
 241 possible effects in larval settlement. Also, given the pen shell distribution along the shallow  
 242 sandbars of the ancient coastline, the edge correction method was used to correct for possible  
 243 underestimations near the edge of the study area.

244 Given the large number of available point features (see next section), a total of 99  
 245 permutations was used to run the model and generate higher and lower confidence envelopes.

246 We used the default program setting including 10 distance bands, with 1 m as initial distance  
247 and increments of 50 m, and the user provided study area feature class available in the tool.

248

### 249 **3. Results**

#### 250 *3.1. Monthly records of salinity and temperature*

251 Monthly averages of salinity during the study (March to July 2021) varied between  $35.7 \pm$   
252  $0.2$  and  $36.1 \pm 0.4$  in the Banya zone (Zone 1) and between  $35.6 \pm 0.2$  and  $36.2 \pm 0.3$  in the  
253 Trabucador (Zone 2). However, salinities above 36.5 (i.e., the lower limit for parasite infection;  
254 Cabanellas-Reboredo et al., 2019) were detected during two consecutive weeks in the Banya  
255 and once in the Trabucador zone, in late July. In the St. Joan Tower (Zone 3), mean monthly  
256 salinities were lower than in outer zones, with values between  $34.7 \pm 0.7$  and  $35.7 \pm 0.2$  during  
257 the study period, with values always below 36.5.

258 For temperature, monthly averages increased from  $14.7 \pm 0.05$  to  $26.5 \pm 0.4$  °C in the Banya  
259 zone (Zone 1), from  $14.6 \pm 0.03$  to  $26.8 \pm 0.8$  °C in the Trabucador (Zone 2), and from  $15.3 \pm$   
260  $0.04$  to  $27.2 \pm 0.7$  °C in the St. Joan Tower (Zone 3) between March and July 2021.

261

#### 262 *3.2. Abundances across study sites*

263 In the Banya Peninsula (Zone 1) a total of 3,137 shells were found within the study area of  
264 4,1 ha. Out of these, 45.9% of individuals were live individuals and the remaining 54.1% were  
265 empty shells (Fig. 2). Among live individuals the majority (81.5%) were large adults, with a  
266 lesser component of young adults (17.1%) and even lower component of juveniles (1.4%). In  
267 the Trabucador (Zone 2), 1,651 shells were recorded within a larger area of 5.7 ha, although  
268 with a similar proportion of live individuals vs. empty shells (51.7 and 48.3%, respectively). The  
269 bulk of the live population were adults (45.3%), and young adults (46.8%), and there was also a  
270 larger component of juveniles than in Zone 1 (7.9%). The St. Joan tower area (Zone 3) hosted  
271 the lowest number of shells (650 pen shells in 4.2 ha), although with a higher proportion of live

272 individuals vs. empty shells (62.2 vs. 37.8%) (Fig. 2). In this zone, live individuals were  
273 dominated by young adults (60.6%), followed by adults (39.4%), with no observation of  
274 juveniles (only 1 individual was found at a very shallow depth but was outside the study area).

275 MANOVA analyses with the size structure of individuals confirmed the presence of  
276 significant differences among the three study areas, consistently for live individuals, empty  
277 shells, and total shells (Table 1A-C; Fig. 3A-C). The Banya zone showed the highest abundance  
278 of live individuals, empty shells, and total shells, followed by the Trabucador, and the St. Joan  
279 Tower zone, with patterns being mostly driven by a greater abundance of large adults. For live  
280 individuals and total shells, young adults in the Banya and Trabucador zones showed similarly  
281 higher abundances than the St. Joan Tower zone, while juveniles were significantly higher in  
282 the Trabucador, and lower in the Banya, and the St. Joan Tower zone, where none was  
283 observed. In contrast, differences in the abundance of empty shells were entirely due to the  
284 presence of large adults (Table 1B, Fig. 3B), which comprised 99.5, 95.6, and 93.5% of empty  
285 shells in the Banya, Trabucador, and St. Joan Tower zones, respectively. Only 23 young adults  
286 and 2 juvenile empty shells were found in the Banya zone, 30 young adults and 5 juveniles in  
287 the Trabucador, and 14 young adults and 1 juvenile in the St. Joan Tower zone. Among  
288 observed empty shells, only 2 adults, 1 young adult and 1 juvenile in the Trabucador were  
289 recent.

290 MANOVA results with habitat groups also evidenced the presence of further significant  
291 differences among sites (Table 1D-F; Fig. 3D-F). The Banya zone hosted most of live individuals  
292 and empty shells, which were significantly more abundant in unvegetated sandy areas (83%  
293 and 77.6% for live individuals and empty shells, respectively); this habitat being comparatively  
294 scarce in the other two zones. The seagrass *C. nodosa* hosted most of the remaining individuals  
295 in the Banya zone (16.8 and 22.3% of live individuals and empty shells), and similar to slightly  
296 lower abundances were observed for individuals in the Trabucador. The St. Joan Tower zone  
297 hosted the highest abundance of individuals in *C. prolifera* (82.1 and 71.1% for live individuals

298 and empty shells), followed by the Trabucador (26.6 and 20.1%, respectively), and negligible in  
299 the investigated area of the Banya Peninsula. The Trabucador zone featured higher  
300 abundances of individuals in mixed habitats of *C. nodosa* and *C. prolifera* (45.4 and 47.6% for  
301 live individuals and empty shells), followed in much lower abundance by the St. Joan Tower  
302 zone (7.4 and 4.9%, respectively).

303 One-way ANOVA results for live individuals, empty shells and total shells confirmed overall  
304 patterns, with higher abundances in the Banya zone, followed by the Trabucador, and lowest  
305 in the St. Joan Tower zone (Table 1G-I; Fig. 3A-C).

306 The depth distribution of individuals also displayed notable differences among sites (Fig.  
307 4A-C). In the Banya Peninsula, individuals were found at depths ranging from 20 to 115 cm,  
308 peaking at 60 to 80 cm for both live individuals and empty shells, and similar ranges (10 to 125  
309 cm) could be also found in the Traducador, although with a broader peak (40 to 80 cm). In  
310 contrast, the St. Joan Tower zone features a deeper distribution, peaking at 120 to 130 cm and  
311 still high abundances of individuals at 175 cm with an unknown depth limit outside the study  
312 area.

313

### 314 3.3. Point patterns analyses

315 Results for the Nearest Neighbor (NN) analyses showed significant clustering patterns  
316 (values < 1) in all study zones (Table 2). Clustering was slightly higher in the Trabucador (Zone  
317 2) than in the central part of the Banya Peninsula (Zone 1), and lowest in the St. Joan Tower  
318 area (Zone 3) which showed the highest NN Ratios and Z Scores, particularly for empty shells.  
319 There was also a remarkable similarity in the NN ratios of live individuals vs. empty shells  
320 evidencing the persistence of spatial patterns over large periods of time. In two of the study  
321 zones, the Banya Peninsula, and the St. Joan Tower observed NN distances were either equal  
322 or larger than those observed for empty shells, respectively (Table 2). In contrast, in the  
323 Trabucador zone NN distances were slightly closer for empty shells than for live individuals.

324 Results for Multi-distance Spatial Cluster Analyses (MDSCA) provided additional information  
325 about the size of the aggregations at greater spatial scales (100s of m). In the Banyas Peninsula  
326 (Zone 1), animals were clustered up to distances of 125 m (live animals), 115 (empty shells),  
327 and 120 m (combined data) when all shells were included in the analysis. In the Trabucador  
328 (Zone 2), clustering patterns reached larger distances ranging from 175 m (live animals) to up  
329 to 190 m (empty shells), and 180 m for combined data. Intermediate values were obtained for  
330 the St. Joan Tower area (Zone 3), where pen shells we clustered until distances of 170 m (live  
331 animals), 140 (empty shells), and 160 m (combined data). Beyond those distances, MDSPA  
332 results evidenced tendency to dispersion. In Zone 1, the significance of these patterns with  
333 respect to the higher and lower confidence envelopes was very little (Fig. 5A-C). In Zone 2, pen  
334 shells showed significant clustering at distances below 100 to 130 m, and significantly  
335 dispersed at distances from ca. 180-190 to 320-360 m in all groups (live individuals, empty  
336 shells, and both combined) (Fig. 5D-F). In contrast, Zone 3, consistently displayed significant  
337 clustering at distances up to ca. 140 to 170 for all groups (live individuals, empty shells, and  
338 combined data) but patterns of dispersion were non-significant at greater distances (Fig. 5G-I).

339

#### 340 **4. Discussion**

341 Our results show that the three study areas of the Alfacs Bay still host (by July 2021) a large  
342 abundance of individuals –a total of 2,697 pen shells found alive in 14 Ha– that constitute one  
343 of the few remaining reservoirs of the species in the Mediterranean, and the largest sanctuary  
344 within Spanish waters. Our findings are comparable to the 2,762 live individuals observed  
345 during 258 visual surveys throughout Greece by 9 research groups, most of them in the Kalloni  
346 Gulf (Lesvos Island) and in Laganas Bay (Zakynthos Island) (Zotou et al., 2020). Yet, the total  
347 size of populations within remaining areas is still unknown. The Alfacs Bay spreads over an  
348 estimated area of ca. 49 km<sup>2</sup>, but the outer half of the bay was severely impacted by the  
349 disease in 2018 (Prado et al., 2021). Besides, the local pen shell distribution seems very

350 restricted to shallow areas, mostly from ca. 20 to 130 cm of water depth, excepting in areas of  
351 the North coast, where it can reach over 175 cm of water (Prado et al., 2014; this study). In the  
352 absence of an accurate bathymetry, we roughly estimate that ca. 500 ha of suitable bay  
353 habitat might remain to be surveyed for population abundance. The three study zones  
354 presented distinctive densities of live individuals ranging from 1,440 (3.5 ind./ 100 m<sup>2</sup>) in the  
355 Banya, 853 (1.5 ind./ 100 m<sup>2</sup>) in the Trabucador, and 404 (0.96 ind./ 100 m<sup>2</sup>) in the St. Joan  
356 Tower zone, which appear to be related to local habitat quality and historical patterns of  
357 recruitment success (Prado et al., 2014, 2020a). The Northern coast of the Alfacs Bay is  
358 immediately adjacent to drainage channels from extensive rice agriculture and reveals signs of  
359 siltation and eutrophication in submerged vegetation (Prado, 2018), that might have negative  
360 effects on respiration and feeding of benthic invertebrates (Thorson, 1950). In fact, the  
361 bathymetric distribution in the St. Joan Tower zone appears to be related to distance from silt  
362 deposit areas as reported elsewhere (Katsanevakis, 2006). In contrast, the Banya Peninsula is  
363 located further away from the source of anthropic influence and closer from the mouth of the  
364 bay region which features a more reduced residence time of water (ca. 5-10 days; Cerralbo et  
365 al., 2019) that allowed connectivity with other populations previously to MMEs (Wesselmann  
366 et al., 2018). Despite such less favorable effects of habitat quality, paradoxically, the proximity  
367 to freshwater discharges provides enhanced protection against the advance of pen shell  
368 disease. Prado et al., (2021) monitored cumulative pen shell mortality in three sites of the  
369 Banya Peninsula and found a positive association with the salinity gradient (37.4 to 35.7), with  
370 higher rates close to the mouth of the bay (100% of individuals) and intermediate (43%) to low  
371 rates (13%) in the middle and inner regions of the Banya Peninsula. During the study (March to  
372 early July 2021) monthly averages of salinity were below the 36.5 low range limit established  
373 for disease transmission (Cabanelas-Reboredo et al., 2019), although with exceptions during  
374 late July (after georeferencing sampling) in the Banya zone (2 consecutive weeks) and in the  
375 Trabucador (1 week), that greatly increase infection risk.



376 The dynamics of disease acquisition and transmission in other organisms such as grapevine  
377 *Vitis vinifera* infected with “flavescence dorée” has evidenced variations in clustering patterns  
378 that were attributed to the temporal spread of the epidemics (Maggi et al., 2017). Also, Gienke  
379 et al., (2014), used point pattern analysis to examine the effect of beech bark disease and  
380 reported enhanced severity – i.e., a clustering effect– in beech saplings located in the  
381 proximity (< 5 m) of highly cankered canopy beech trees. In contrast, our results for NN  
382 analysis showed a general similarity in patterns of aggregation between live individuals and  
383 empty shells, that coupled with scarce recent mortality in all zones (0.15% of total empty  
384 shells) points to a disease-free scenario within study zones. Yet, slightly lower NN ratios in  
385 empty shells occurred in the Trabucador zone (i.e., higher clustering) resulting in lower NN  
386 distances which suggest the trace of a previous outbreak. In fact, the area was directly  
387 connected with the open sea during a ca. 4-month period due to breakage of the Trabucador  
388 sand bar during the Gloria Storm from January to May 2020 (Pintó i Fusalba et al., 2020).  
389 Samples from five juveniles found by fishermen in the outer sea just in front of the Trabucador  
390 sand bar during that period were all found to be positive to the parasite by PCR (G. Catanese,  
391 pers. comm.) and reinforce the possible entrance of the disease and a subsequent  
392 stabilization. Besides, MDSCA for the Trabucador also evidenced clustering effects at greater  
393 distances in empty shells than in live individuals (190 vs. 175 m) further supporting the  
394 occurrence of previous disease effects. Both NN and MDSCA showed enhanced clumping of  
395 hosts in the Trabucador zone, which be a relevant factor limiting the advance of a disease  
396 vector during the initial phase of an epidemic process (Caraco et al., 2001). Conversely, both  
397 the Banya Peninsula and the St. Joan Tower showed greater larger aggregation in live  
398 individuals (by 10 and 30 m, respectively). For the Banya Peninsula this apparent absence of  
399 disease effects contrast with the 43% mortality observed in middle regions by Prado et al.,  
400 (2021). Yet, monitoring circles were located ca. 250 m beyond the end of the assessed area,  
401 pointing that this middle zone of the bay marks the transition from more affected to less

402 affected areas. Besides, given the large dominance of large adults in the area, an effect of  
403 increased natural mortality cannot be discarded given the low age expectancy of Alfacs Bay  
404 individuals (dominance of the  $8 \pm 1$  year-old class and a maximum age of 15 years; Prado et al.,  
405 2020a). In fact, the abundance of empty shells (ca. 54.1%, 48.3%, and 37.8% of the total shells  
406 observed in the Banya, Trabucador, and St. Joan Tower zones, respectively) was completely  
407 biased towards large adults, which comprised up to 97.3% of the total, with only a minor  
408 component of young adults and juveniles (2.4 and 0.3%, respectively). Since that the Banya  
409 zone hosted a size distribution with a greater component of adults than the other investigated  
410 zones (90.7% vs. 70.1 and 60%), higher mortality could be mostly attributed to the presence of  
411 older size classes. Alternatively, an enhanced disappearance of younger, brittle shells, could  
412 also be possible, but is not supported by recruitment surveys and annual deployment of  
413 collectors in the Alfacs Bay from 2016 (Prado et al., 2019; Kersting et al., 2020).

414 The relative similarity in MDSCA clustering patterns across the three study zones featuring  
415 contrasting types of dominant benthic habitats (sand in the Banya zone, mixed vegetation in  
416 the Trabucador, and *Caulerpa* in the St. Joan Tower), also suggest the absence of preferential  
417 habitat settlement, as reported for some species of bivalves such as the Northern quahog  
418 *Mercenaria mercenaria* (Bachelet et al., 1992) or the Mediterranean mussel *Mytilus*  
419 *galloprovincialis* (Cáceres-Martínez et al., 1994). Effects of differential habitat mortality are  
420 considered unlikely due to considerably higher presence of individuals in bare sandy patches of  
421 the Banya Peninsula, which would have facilitated access to local predators such as decapods,  
422 cephalopods and fishes, and the gastropod *Hexaples trunculus*, at lengths < 45 cm (refuge size)  
423 compared to enhanced protection provided by vegetated areas (Farina et al., 2009, García-  
424 March et al., 2007; Kersting & García-March, 2017). Alternatively, they could be the combined  
425 result of a limited dispersal capacity of oocytes and larvae from the emission source, local  
426 circulation, and coastal geomorphology features. Oocytes of *P. nobilis* have been indicated a  
427 low buoyancy and a tendency to sink (Trigos et al., 2018), and the mobility of the D-larvae also

428 appears to be lower than in other bivalves (P. Prado, personal observ.), which might constrict  
429 dispersal in confined waters. Besides, according to Cerralbo et al., (2019), water residence time  
430 in middle to inner parts of the Alfacs Bay embracing the three study zones ranges from 35 to  
431 45 days; a considerably longer period than the expected planktonic duration of *P. nobilis* larvae  
432 (Trigos et al., 2018) and may favor local recruitment in favorable years. Another important  
433 factor responsible for aggregation appear to be the presence of very shallow sand bars –  
434 remains of the ancient coastline–, acting as a physical barrier for larval dispersal towards the  
435 coast (Prado et al., 2020a). Their presence explains the distribution of pen shells along belt  
436 areas parallel to shore and the tendency towards disperse patterns at larger scales in all zones.  
437 Compared to other bivalves where clustering in dense matts or reefs are the result of selective  
438 settlement patterns (Grassle et al., 1992; Vasquez et al., 2013), those of the pen shell appear  
439 to be due to an early life-stage strategy based on low buoyancy and passive drift. The possible  
440 effect of parental detection in larval settlement cannot be fully discarded, but there was  
441 considerable variability in mean NN distances to another shell across zones (from only 1.2 in  
442 the Banya to 3.1 m in the St. Joan Tower), which suggest that adult proximity is not a necessary  
443 requirement.

444 The age structure of the live pen shell population in the Alfacs Bay was dominated by adult  
445 and young adult individuals, although with significant differences among study sites. Older  
446 individuals with greater size were dominant in the Banya Peninsula (8.15%), whereas in the  
447 Trabucador and the St. Joan Tower, there were increasing numbers of young adults (46.8 vs.  
448 45.2% and 60.6 vs. 39.3%, respectively for each age size and zone), evidencing that  
449 recruitment events are sparse and not homogeneous within the bay. The overall juvenile  
450 abundance was very low across the different zones, with values close to zero in the St. Joan  
451 Tower and the Banya zone (0 to 1.4%) but higher in the Trabucador (7.9%), which is  
452 comparable to local spatial variability observed in other studies (e.g., Giménez-Casaldueiro et  
453 al., 2020; Katsanevakis 2006; García-March et al., 2007). Yet, considering the potentially large

454 size of the remaining population (only discrete bay areas were counted), the presence of  
455 juveniles was surprisingly low; to some extent, some individuals could have been overlooked in  
456 dense canopy areas but their absence in bare sand areas of the Banya Peninsula where adults  
457 were very abundant cannot be misleading. A single pen shell female may release in the order  
458 of tens of millions of eggs for reproduction (Trigos et al., 2018), thus supposedly conferring an  
459 enormous reproductive potential to the Alfacs Bay population. Conversely, recruitment  
460 patterns inferred from shell growth records of the posterior adductor muscle suggest window  
461 periods of up to 11 years between successive events (Prado et al., 2020a), which is  
462 considerably long compared to the more even size structure usually reported in open water  
463 populations (García-March et al., 2020a). The reasons for this mismatch between spawning  
464 potential and effective recruitment are yet unclear. In open water populations, predation  
465 mortality has been proposed as a key factor explaining differences between larval supply and  
466 recruitment patterns before MMEs (Kersting & García-March, 2017). Yet, the Alfacs Bay  
467 appears to feature a low availability of pen shell larvae throughout the summer (Andree et al.,  
468 2018) and recent research both in lab and in the wild points out to the occurrence of a single,  
469 main spawning event during the month of May at temperatures ranging between ca. 19-23 °C  
470 (P. Prado, personal observ.). Besides, repeated unsuccessful attempts to close the life cycle in  
471 captivity using local individuals suggest the undergoing of other factors. First, Prado et al.,  
472 (2020a) proposed that the presence of simultaneous hermaphroditism –a condition that has  
473 been associated with pollution and environmental stress– could lead to in-breeding depression  
474 and potentially reduced fertility. Other possible mechanism could be the occurrence of high  
475 local inbreeding causing enhanced number of deleterious mutations and consequently  
476 reducing fitness in the offspring of highly fecund marine animals (see Plough, 2016). For  
477 instance, recent work in the Pacific oyster, *Crassostrea gigas*, has shown that genetic  
478 unviability is a major factor driving early life mortality in hatchery and field environments  
479 (Plough et al., 2016), and is currently being investigated for *P. nobilis*.

480

## 481 **5. Conclusion**

482 Point pattern analysis provided integrative information on population condition and disease  
483 outbreaks at several temporal scales. During the study period, the three study zones displayed  
484 an apparent absence of disease symptoms but point pattern analysis (both NN and MDSCA)  
485 evidenced enhanced clustering of empty shells in the Trabucador zone, which suggest a  
486 previous disease condition and was likely slowed or adjourned after the reconstruction of the  
487 Trabucador sandbar and the reestablishment of normal conditions with lower salinity (Prado  
488 et al., 2021). Aside the Alfacs Bay, surviving populations are also known to exist in confined  
489 waters of the Mar Menor Lagoon in Spain (Giménez-Casalduero et al., 2020), the Diana Lagoon  
490 in Corse (Simide et al., 2019), the Salses-Leucate, and Thau lagoons in the Gulf of Lion, France  
491 (Peyran et al., 2021), the Venice lagoon in Italy (Russo 2017), the Kalloni Gulf (Lesvos Island),  
492 and Laganas Bay (Zakynthos Island) in Greece (Zotou et al., 2020) among other possible  
493 locations. Yet, survival might be ephemeral without adequate monitoring and management  
494 programs. For instance, one of the last fortresses of the species in the Marmara Sea in Turkey  
495 appear to have been recently infected and largely lost over a period of only few months (Cinar  
496 et al., 2021a, b), pointing out the need of effective monitoring tools to guide conservation  
497 actions such as translocation of animals to aquarium facilities now that robust protocols for  
498 captivity maintenance have been developed (Hernandis et al., in prep). Uninfected animals  
499 could be also moved to other natural areas or regions with lower infection risk. Besides, in  
500 some locations such as the Alfacs Bay, the proximity of agricultural discharge channels could  
501 allow the additional release of freshwater during periods of high risk due to increased summer  
502 salinities. This action could particularly benefit the conservation of pen shells in middle regions  
503 of the Banya Peninsula and the Trabucador, which are sometimes above the lower salinity  
504 threshold for parasite infection at 36.5 and might experience an intermittent spread of the  
505 disease. Besides, it could also be implemented to preserve estuarine conditions in case of new

506 breakage of the Trabucador sand bar during heavy storms —such as the Gloria Storm in 2020  
507 (Pintó i Fusalba et al., 2020)—, as foreseen by severe thinning over the last decade. Infection  
508 risk also needs to be put in the context of the low presence of juveniles observed in the bay –  
509 the last large recruitment was observed in 2017 (Prado et al., 2020a)—, thus making essential  
510 the long-term maintenance of populations to allow new recruitment events. There is an  
511 imperative need for compromise from the public administrations to start implementing  
512 management actions based on proposed scientific evidence to preserve the last remaining  
513 sanctuaries of *P. nobilis*.

514

#### 515 **Acknowledgements**

516 Authors are grateful to the Biodiversity Foundation of the Ministry for Ecological Transition  
517 and the Demographic Challenge for supporting the Recupera Pinna project in the 2020 call for  
518 proposals. P. Prado was contracted under the INIA-CCAA cooperative research program for  
519 postdoctoral incorporation from the Spanish National Institute for Agricultural and Food  
520 Research and Technology (INIA). Authors would like to thank the Corps of Rural Agents (CAR)  
521 for technical assistance during fieldwork sampling. Further field support was provided also by  
522 Eric Rives, Mireia Salvadó, Josep Xarles Ribas, Jose Luis Costa, Lluís Jornet, and David Mateu.

523

524 **References**

- 525 Andree, K. B., Trigos, S., Vicente, N., Carrasco, N., Carella, F., Prado, P. (2018). Identification of  
526 potential recruitment bottlenecks in larval stages of the giant fan mussel *Pinna nobilis* using  
527 specific quantitative PCR. *Hydrobiologia*, 818(1), 235–247. [https://doi.org/10.1007/s10750-](https://doi.org/10.1007/s10750-018-3616-x)  
528 018-3616-x
- 529 Bachelet, G., Butman, C. A., Webb, C. M., Starczak, V. R., Snelgrove, P. V. (1992). Non-selective  
530 settlement of *Mercenaria mercenaria* (L) larvae in short-term still-water laboratory  
531 experiments. *Journal of Experimental Marine Biology and Ecology*, 161, 241–280.  
532 [https://doi.org/10.1016/0022-0981\(92\)90100-O](https://doi.org/10.1016/0022-0981(92)90100-O)
- 533 Basso, L., Vázquez-Luis, M., García-March, J. R., Deudero, S. et al. (2015). The pen shell *Pinna*  
534 *nobilis*: A review of population status and recommended research priorities in the  
535 Mediterranean Sea. *Advances in Marine Biology*, 71, 109–160.  
536 <https://doi.org/10.1016/bs.amb.2015.06.002>
- 537 Berntsson, K. M., Jonsson, P. R., Larsson, A. I., Holdt, S. (2004). Rejection of unsuitable  
538 substrata as a potential driver of aggregated settlement in the barnacle *Balanus improvisus*.  
539 *Marine Ecology Progress Series*, 275, 199-210. <http://www.jstor.org/stable/24867679>
- 540 Brooks, J. W. (2016). Postmortem changes in animal carcasses and estimation of the  
541 postmortem interval. *Veterinary Pathology*, 53 (5), 929–940.  
542 <https://doi.org/10.1177/0300985816629720>
- 543 Cabanellas-Reboredo, M., Vázquez-Luis, M., Mourre, B., Álvarez, E., et al. (2019). Tracking a  
544 mass mortality outbreak of pen shell *Pinna nobilis* populations: a collaborative effort of  
545 scientists and citizens. *Scientific Reports*, 9, 1–11. [https://doi.org/10.1038/s41598-019-](https://doi.org/10.1038/s41598-019-49808-4)  
546 49808-4
- 547 Cáceres–Martínez, J., Robledo, J. A., Figueras, A. (1994). Settlement and post–larvae behaviour  
548 of *Mytilus galtoprovincialis*: field and laboratory experiments. *Marine Ecology Progress*  
549 *Series*, 112, 107–117.

550 Caraco, T., Duryea, M. C., Glavanakov, S., Maniatty, W., Szymanski, B. K. (2001). Host spatial  
551 heterogeneity and the spread of vector-borne infection. *Theoretical Population Biology*, 59  
552 (3), 185–206. <https://doi.org/10.1006/tpbi.2000.1517>

553 Carella, F., Aceto, S., Pollaro, G., Miccio, A., et al. (2019). A mycobacterial disease is associated  
554 with the silent mass mortality of the pen shell *Pinna nobilis* along the Tyrrhenian coastline  
555 of Italy. *Scientific Reports*, 9, 2725. <https://doi.org/10.1038/s41598-018-37217-y>

556 Carella, F., Elisabetta, A., Simone, F., Fulvio, S., et al. (2020). In the wake of the ongoing mass  
557 mortality events: Co-occurrence of *Mycobacterium*, *Haplosporidium* and other pathogens  
558 in *Pinna nobilis* collected in Italy and Spain Mediterranean Sea. *Frontiers in Marine Science*,  
559 7, 48. [doi.org/10.3389/fmars.2020.00048](https://doi.org/10.3389/fmars.2020.00048)

560 Catanese, G., Grau, A., Valencia, J. M., Garcia-March, J.R., et al. (2018). *Haplosporidium pinnae*  
561 sp. nov., a haplosporidan parasite associated with mass mortalities of the fan mussel *Pinna*  
562 *nobilis* in the Western Mediterranean Sea. *Journal of Invertebrate Pathology*, 157, 9–24.  
563 <https://doi.org/10.1016/j.jip.2018.07.006>

564 Cerralbo, P., Pedrera Balsells, M. F., Mestres, M., Fernandez, M., et al. (2019). Use of a  
565 hydrodynamic model for the management of water renovation in a coastal system. *Ocean*  
566 *Science*, 15, 215–226. <https://doi.org/10.5194/os-15-215-201>

567 Clark, P. J., Evans, F. C. (1954). Distance to nearest neighbor as a measure of spatial  
568 relationships in populations. *Ecology*, 35, 445–453. <https://doi.org/10.2307/1931034>

569 Cinar, M.E., Bilecenoğlu, M., Yokeş, M. B., Güçlüsoy, H. (2021a). *Pinna nobilis* in the south  
570 Marmara Islands Sea of Marmara.; it still remains uninfected by the epidemic and acts as  
571 egg laying substratum for an alien invader. *Mediterranean Marine Science*, 22, 161–168.  
572 <https://doi.org/10.12681/mms.25289>

573 Cinar, M. E., Bilecenoğlu, M., Yokeş, M. B., Güçlüsoy, H. (2021b). The last fortress fell: mass  
574 mortality of *Pinna nobilis* in the Sea of Marmara. *Mediterranean Marine Science*, 22(3),  
575 669–676. <https://doi.org/10.12681/mms.27137>



576 Cox, K. D., Black, M. J., Filip, N., Miller, M. R., et al. (2017). Community assessment techniques  
577 and the implications for rarefaction and extrapolation with Hill numbers. *Ecology and*  
578 *Evolution*, 7, 11213–11226. <https://doi.org/10.1002/ece3.3580>

579 Dixon, P. M. (2002). Nearest neighbor methods. *Encyclopedia of environmetrics*, 3, 1370–1383.

580 Farina, S., Tomas, F., Prado, P., Romero, J., Alcoverro, T. (2009). Seagrass meadow structure  
581 alters interactions between the sea urchin *Paracentrotus lividus* and its predators. *Marine*  
582 *Ecology Progress Series*, 377, 131–137. <https://doi.org/10.3354/meps07692>

583 García-March, J.R., García-Carrascosa, A. M., Peña Cantero, A. P., Wang, Y. G. (2007).  
584 Population structure mortality and growth of *Pinna nobilis* Linnaeus 1758 Mollusca Bivalvia.  
585 at different depths in Moraira bay (Alicante Western Mediterranean). *Marine Biology*, 150,  
586 861–871. <https://doi.org/10.1007/s00227-006-0386-1>

587 García-March, J. R., Hernandis, S., Vázquez-Luis, M., Prado, P., et al. (2020a). Age and growth  
588 of the endangered fan mussel *Pinna nobilis* in the western Mediterranean Sea. *Marine*  
589 *Environmental Research*, 153, 104795. <https://doi.org/10.1016/j.marenvres.2019.104795>

590 García-March, J. R., Tena, J., Henandis, S., Vázquez-Luis, M., et al. (2020b). Can we save a  
591 marine species affected by a highly infective highly lethal waterborne disease from  
592 extinction?. *Biological Conservation*, 243, 108498.  
593 <https://doi.org/10.1016/j.biocon.2020.108498>

594 Giencke, L. M., Dovčiak, M., Mountrakis, G., Cale, J. A., Mitchell, M. J. (2014). Beech bark  
595 disease: spatial patterns of thicket formation and disease spread in an aftermath forest in  
596 the northeastern United States. *Canadian Journal of Forest Research*, 44(9), 1042–1050.  
597 <https://doi.org/10.1139/cjfr-2014-0038>

598 Giménez-Casalduero, F., Gomariz-Castillo, F., Alonso-Sarría, F., Cortés, E., Izquierdo-Muñoz, A.,  
599 Ramos, A. (2020). *Pinna nobilis* in the Mar Menor coastal lagoon: a story of colonization and  
600 uncertainty. *Marine Ecology Progress Series*, 652, 77–94.  
601 <https://doi.org/10.3354/meps13468>

602 Gosselin, L. A., Qian, P. Y. (1997). Juvenile mortality in benthic marine invertebrates. *Marine*  
603 *Ecology Progress Series*, 146, 265–282. <https://doi.org/10.3354/meps146265>

604 Grassle, J. P., Snelgrove, P. V., Butman, C. A. (1992). Larval habitat choice in still water and  
605 flume flows by the opportunistic bivalve *Mulinia lateralis*. *Netherland Journal of. Sea*  
606 *Research*, 30, 33–44. [https://doi.org/10.1016/0077-7579\(92\)90043-E](https://doi.org/10.1016/0077-7579(92)90043-E)

607 Haase, P., Pugnaire, F. I., Clark, S. C., Incoll, L. D. (1996). Spatial patterns in a two-tiered semi-  
608 arid shrubland in southeastern Spain. *Journal of Vegetation Science*, 7(4), 527-534.  
609 <https://doi.org/10.2307/3236301>

610 Hamill, D. N., Wright, S. J. (1986). Testing the dispersion of juveniles relative to adults: A new  
611 analytic method: Ecological Archives E067-004. *Ecology*, 67, 952–957.  
612 <https://doi.org/10.2307/1939817>

613 He, F., Duncan, R. P. (2000). Density-dependent effects on tree survival in an old-growth  
614 Douglas fir forest. *Journal of Ecology*, 88, 676–688. [https://doi.org/10.1046/j.1365-](https://doi.org/10.1046/j.1365-2745.2000.00482.x)  
615 [2745.2000.00482.x](https://doi.org/10.1046/j.1365-2745.2000.00482.x)

616 Hoffmann, V., Pfaff, M. C., Branch, G. M. (2012). Spatio-temporal patterns of larval supply and  
617 settlement of intertidal invertebrates reflect a combination of passive transport and larval  
618 behavior. *Journal of Experimental Marine Biology, and Ecology*, 418, 83–90.  
619 <https://doi.org/10.1016/j.jembe.2012.03.008>

620 Huang, X., Xiong, G., Chen, X., Liu, R., et al. (2021). Autolysis in crustacean tissues after death:  
621 A case study using the *Procambarus clarkii* hepatopancreas. *BioMedical Research*  
622 *International*. <https://doi.org/101155/2021/2345878>

623 Hunt, H. L., Scheibling, R. E. (1997). Role of early post-settlement mortality in recruitment of  
624 benthic marine invertebrates. *Marine Ecology Progress Series*, 155, 269–301.  
625 <https://doi.org/10.3354/meps155269>

626 Katsanevakis, S. (2006). Population ecology of the endangered fan mussel *Pinna nobilis* in a  
627 marine lake. *Marine Ecology Progress Series*, 1, 51–59. <https://doi.org/10.3354/esr001051>

628 Katsanevakis, S., Carella, F., Çinar, M. E., Čížmek, H., et al. (2021). The Fan Mussel *Pinna nobilis*  
629 on the brink of extinction in the Mediterranean. *Reference Module in Earth Sciences and*  
630 *Environmental Systems*. <https://doi.org/10.1016/B978-0-12-821139-7.00070-2>

631 Kenkel, N. C. (1988). Pattern of self-thinning in jack pine: testing the random mortality  
632 hypothesis. *Ecology*, 69, 1017–1024. <https://doi.org/10.2307/1941257>

633 Kersting, D., Benabdi, M., Čížmek, H., Grau, A., et al. (2019). *Pinna nobilis*. The IUCN Red List of  
634 Threatened Species 2019: e.T160075998A160081499.  
635 <https://doi.org/10.2305/IUCN.UK.2019-3.RLTS.T160075998A160081499.en>

636 Kersting, D. K., García-March, J. R. (2017). Long-term assessment of recruitment early stages  
637 and population dynamics of the endangered Mediterranean fan mussel *Pinna nobilis* in the  
638 Columbretes Islands (NW Mediterranean). *Marine Environmental Research*, 130, 282–292.  
639 <https://doi.org/10.1016/j.marenvres.2017.08.007>

640 Kersting, D. K., Vázquez-Luis, M., Mourre, B., Belkhamssa, F. Z., et al. (2020). Recruitment  
641 disruption and the role of unaffected populations for potential recovery after the *Pinna*  
642 *nobilis* mass mortality event. *Frontiers in Marine Science*, 882.  
643 <https://doi.org/10.3389/fmars.2020.594378>

644 Kingsford, M. J., Leis, J. M., Shanks, A., Lindeman, K. C., Morgan, S. G., Pineda, J. (2002).  
645 Sensory environments larval abilities and local self-recruitment. *Bulletin of Marine Science*,  
646 70, 309–340.

647 Künili, İ. E., Ertürk Gürkan, S., Aksu, A., Turgay, E., et al. (2021). Mass mortality in endangered  
648 fan mussels *Pinna nobilis* Linnaeus 1758. Caused by co-infection of *Haplosporidium pinnae*  
649 and multiple *Vibrio* infection in Çanakkale Strait, Turkey. *Biomarkers*, 1–12.  
650 <https://doi.org/10.1080/1354750X.2021.1910344>

651 Lattos, A., Bitchava, K., Giantsis, I.A., Theodorou, J.A., Batargias, C., Michaelidis, B. (2021). The  
652 implication of *Vibrio* bacteria in the winter mortalities of the critically endangered *Pinna*  
653 *nobilis*. *Microorganisms*, 9, 922. <https://doi.org/10.3390/microorganisms9050922>

654 Little, L. R., Dale, M. T. R. (1999). A method for analysing spatio-temporal pattern in plant  
655 establishment tested on a *Populus balsamifera* clone. *Journal of Ecology*, *87*, 620–627.  
656 <https://doi.org/10.1046/j.1365-2745.1999.00378.x>

657 Liu, C. (2001). A comparison of five distance-based methods for spatial pattern analysis.  
658 *Journal of Vegetation Science*, *12*, 411–416. <https://doi.org/10.2307/3236855>

659 Maggi, F., Bosco, D., Galetto, L., Palmano, S., Marzachi, C. (2017). Space–time point pattern  
660 analysis of flavescence dorée epidemic in a grapevine field: disease progression and  
661 recovery. *Frontiers in Plant Science*, *7*, 1987. <https://doi.org/10.3389/fpls.2016.01987>

662 Mihaljević, Ž., Pavlinec, Ž., Zupičić, I.G., Oraić, D., et al. (2021). Noble Pen Shell (*Pinna nobilis*)  
663 Mortalities along the Eastern Adriatic Coast with a study of the spreading velocity. *Journal*  
664 *of Marine Science and Engineering*, *9* (7), 764. <https://doi.org/10.3390/jmse9070764>

665 Moeur, M. (1997). Spatial models of competition and gap dynamics in old–growth *Tsuga*  
666 *heterophylla/Thuja plicata* forests. *Forest Ecology and Management*, *94*, 175–186.  
667 [https://doi.org/10.1016/S0378-1127\(96\)03976-X](https://doi.org/10.1016/S0378-1127(96)03976-X)

668 Peyran, C., Boissin, E., Morage, T., Nebot-Colomer, E., et al. (2021). Genetic homogeneity of  
669 the critically endangered fan mussel *Pinna nobilis* throughout lagoons of the Gulf of Lion  
670 (North-Western Mediterranean Sea). *Scientific Reports*, *11*, 1–12.  
671 <https://doi.org/10.1038/s41598-021-87493-4>

672 Pintó i Fusalba, J., Garcia-Lozano, C., Sardá Borroy, R., Roig i Munar, F. X., Martí, C. (2020).  
673 Efectes del temporal Glòria sobre el litoral. *Treballs de la Societat Catalana de Geografia*,  
674 *89*, 89–109. <https://doi.org/10.2436/20.3002.01.192>

675 Plough, L. V. (2016). Genetic load in marine animals: a review. *Current Zoology*, *62*, 567–579.

676 Plough, L. V., Shin, G., Hedgecock, D. (2016). Genetic inviability is a major driver of type III  
677 survivorship in experimental families of a highly fecund marine bivalve. *Molecular Ecology*,  
678 *25*, 895–910. <https://doi.org/10.1093/cz/zow096>

679 Prado, P. (2018). Seagrass epiphytic assemblages are strong indicators of agricultural discharge  
680 but weak indicators of host features. *Estuarine Coastal and Shelf Science*, 204, 140–148.  
681 <https://doi.org/10.1016/j.ecss.2018.02.026>

682 Prado, P., Andree, K. B., Trigos, S., Carrasco, N., et al. (2020a). Breeding planktonic and  
683 settlement factors shape recruitment patterns of one of the last remaining major  
684 population of *Pinna nobilis* within Spanish waters. *Hydrobiologia*, 847, 771–786.  
685 <https://doi.org/10.1007/s10750-019-04137-5>

686 Prado, P., Caiola, N., Ibáñez, C. (2014). Habitat use by a large population of *Pinna nobilis* in  
687 shallow waters. *Scientia Marina*, 78(4), 555–565.  
688 <https://doi.org/10.3989/scimar.04087.03A>

689 Prado, P., Carrasco, N., Catanese, G., Grau, A., et al. (2020b). Presence of *Vibrio mediterranei*  
690 associated to major mortality in stabled individuals of *Pinna nobilis* L. *Aquaculture*, 519,  
691 734899. <https://doi.org/10.1016/j.aquaculture.2019.734899>

692 Prado, P., Grau, A., Catanese, G., Cabanes, P. et al. (2021). *Pinna nobilis* in suboptimal  
693 environments are more tolerant to disease but more vulnerable to severe weather  
694 phenomena. *Marine Environmental Research*, 163, 105220.  
695 <https://doi.org/10.1016/j.marenvres.2020.105220>

696 Prado, P., Tomas, F., Pinna, S., Farina, S. et al. (2012). Habitat and scale shape the demographic  
697 fate of the keystone sea urchin *Paracentrotus lividus* in Mediterranean macrophyte  
698 communities. *PloS one*, 7, e35170. <https://doi.org/10.1371/journal.pone.0035170>

699 Rejmánek, M., Lepš, J. (1996). Negative associations can reveal interspecific competition and  
700 reversal of competitive hierarchies during succession. *Oikos*, 76, 161–168.  
701 <https://doi.org/10.2307/3545758>

702 Ripley, B.D. (1977). Modelling spatial patterns. *Journal of the Royal Statistical Society: Series B*  
703 *(Statistical Methodology)*, 39, 172–212. [https://doi.org/10.1111/j.2517-](https://doi.org/10.1111/j.2517-6161.1977.tb01615.x)  
704 [6161.1977.tb01615.x](https://doi.org/10.1111/j.2517-6161.1977.tb01615.x)

705 Rodríguez, S., Balboa, S., Oliveira, G., Montes, J. et al. (2018). First report of mass mortalities in  
706 natural population of *Pinna nobilis* A microbial perspective. The 7<sup>th</sup> Congress of European  
707 Microbiologists (FEMS 2018).

708 Rozas, V., Camarero, J. J. (2005). Técnicas de análisis espacial de patrones de puntos aplicadas  
709 en ecología forestal. *Investigación agraria: Sistemas y recursos forestales*, 14(1), 79–97.

710 Russo, P. (2017). Lagoon malacofauna, results of malacological research in the Venice Lagoon.  
711 *Bollettino malacologico*, 53, 49–62.

712 Šarić, T., Župan, I., Aceto, S., Villari, G., Palić, D., De Vico, G., Carella, F. (2020). Epidemiology of  
713 noble pen shell (*Pinna nobilis* L. 1758) mass mortality events in adriatic sea is characterised  
714 with rapid spreading and acute disease progression. *Pathogens*, 9(10), 776.  
715 <https://doi.org/10.3390/pathogens9100776>

716 Simide, R., Couvray, S., Vicente, N. (2019). Présence de *Pinna nobilis* L 1758. Dans l'étang  
717 littoral de Diana Corse. *Marine Life Review*, 1–4.

718 Thorson, G. (1950) Reproductive and larval ecology of marine bottom invertebrates. *Biological*  
719 *Reviews*, 25(1), 1–45.

720 Trigos, S., Vicente, N., Prado, P., Espinós, F. J. (2018). Adult spawning and early larval  
721 development of the endangered bivalve *Pinna nobilis*. *Aquaculture*, 483, 102–110.  
722 <https://doi.org/10.1016/j.aquaculture.2017.10.015>

723 Vasquez, H. E., Hashimoto, K., Yoshida, A., Hara, K., et al. (2013). A glycoprotein in shells of  
724 conspecifics induces larval settlement of the Pacific oyster *Crassostrea gigas*. *PloS one*, 8,  
725 e82358. <https://doi.org/10.1371/journal.pone.0082358>

726 Wesselmann, M., González-Wangüemert, M., Serrão, E. A., et al. (2018). Genetic and  
727 oceanographic tools reveal high population connectivity and diversity in the endangered  
728 pen shell *Pinna nobilis*. *Scientific reports*, 8(1), 1-11. [https://doi.org/10.1038/s41598-018-](https://doi.org/10.1038/s41598-018-23004-2)  
729 23004-2

730 Woodin, S.A. (1986). Settlement of infauna: larval choice?. *Bulletin of Marine Science*, 39, 401–  
731 407.

732 Zotou, M., Gkrantounis, P., Karadimou, E., Tsirintanis, K., et al. (2020). *Pinna nobilis* in the  
733 Greek seas NE Mediterranean: on the brink of extinction?. *Mediterranean Marine Science*,  
734 21, 575–591. <https://doi.org/10.12681/mms.23777>

735 **Fig. 1.** Map of the Alfacs Bay showing the location of the 3 study areas where live individuals of  
736 *P. nobilis* can still be found.

737

738 **Fig. 2.** Maps showing the position of live individuals (green dots) and empty shells (red dots)  
739 and the limits of the study area. A) Banya Peninsula (Zone 1); B) Trabucador (Zone 2); and C)  
740 St. Joan Tower (Zone 3).

741

742 **Fig. 3.** Pen shell abundances (mean  $\pm$  SE) within 1,000 m<sup>2</sup> transects at the three study sites. A-  
743 C) Size class abundances (adults= A, young adults= YA, and juveniles= J) for live individuals,  
744 empty, and total pen shells; and D-F) habitat abundances (sand= SA, Caulerpa= C, seagrass= SE,  
745 and mixed vegetation= MV) also for each status and total number of shells.

746

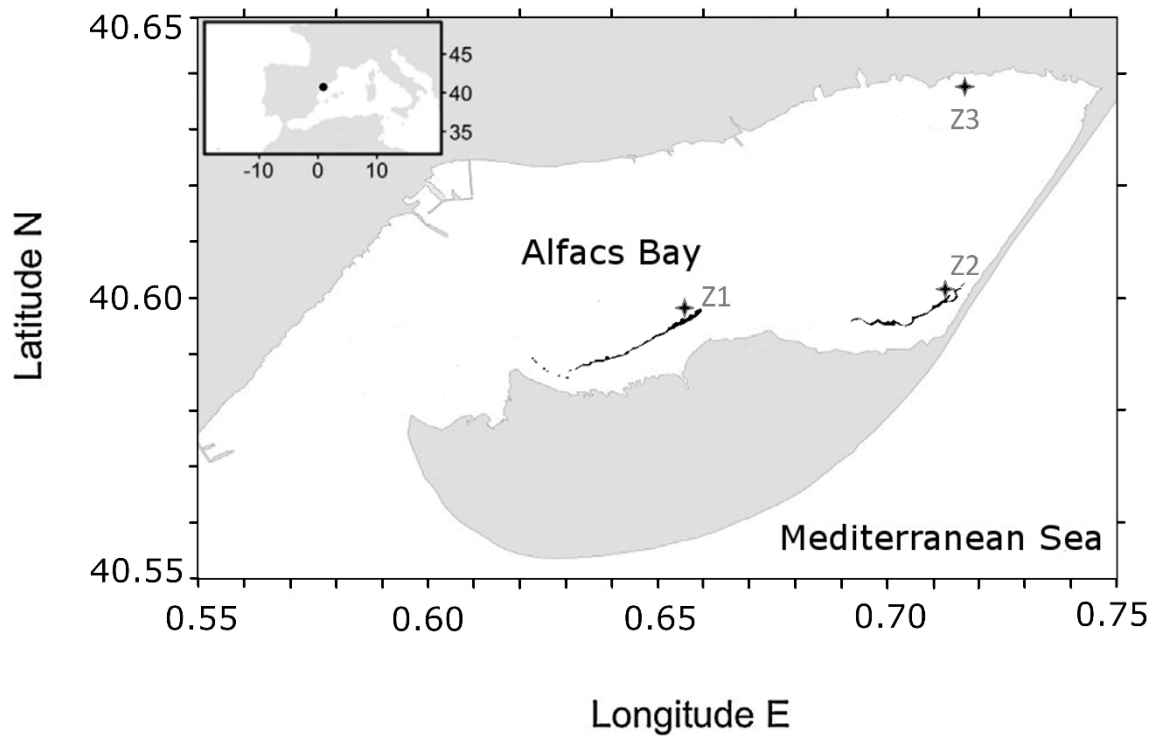
747 **Fig. 4.** Results of MDSCA showing observed vs. expected patterns of clustering and aggregation  
748 at increasing distances (for further details see the M and M section) at each study site. A-C)  
749 Banya Peninsula: live individuals, empty and total shells, respectively; D-F) Trabucador; and G-  
750 I) St. Joan Tower, also respectively for each status and total shells. The high and low  
751 confidence envelopes are also indicated.

752

753 **Fig. 5.** Depth distribution of live individuals and empty shells by study site. A) Banya Peninsula;  
754 B) Trabucador; and C) St. Joan Tower.

755



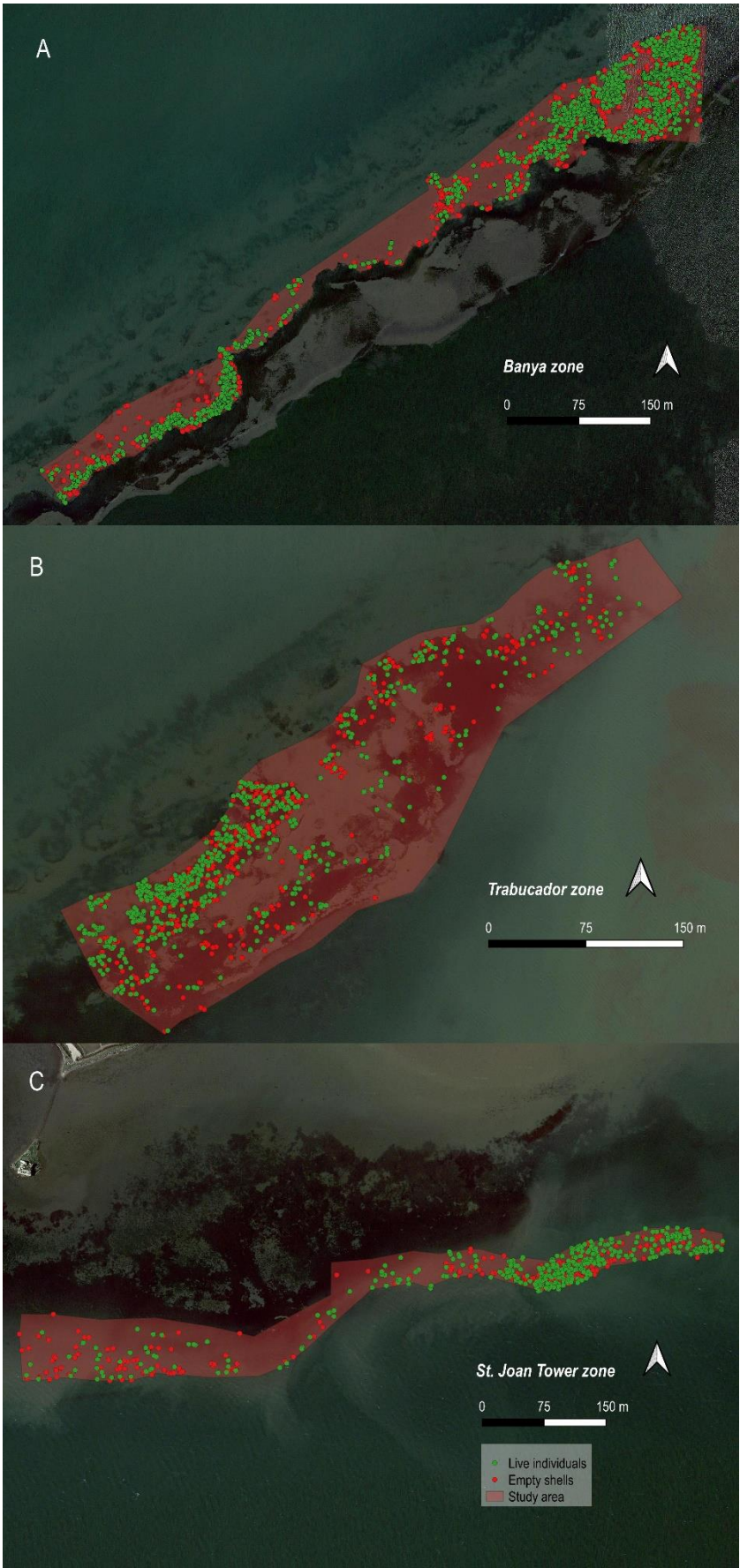


756

757

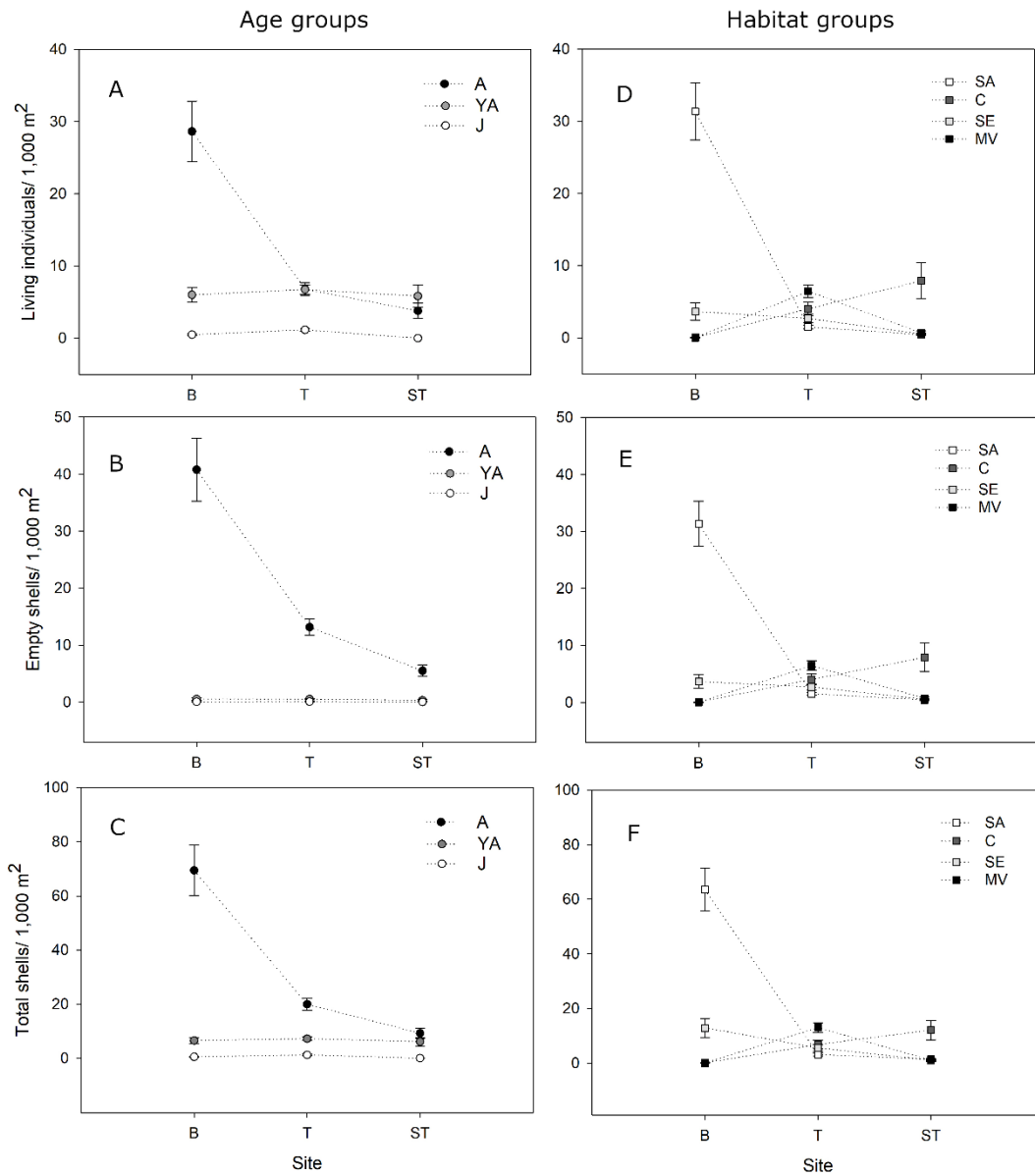
758 Fig. 1.

759



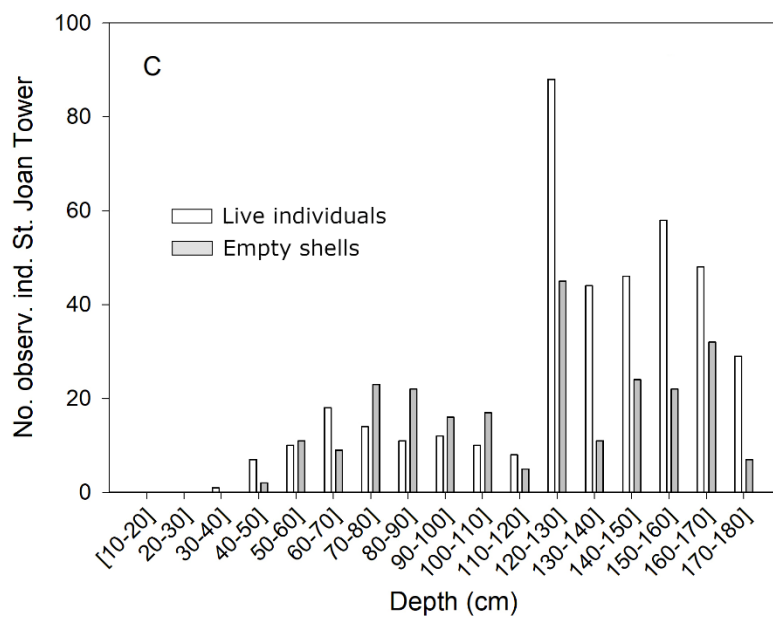
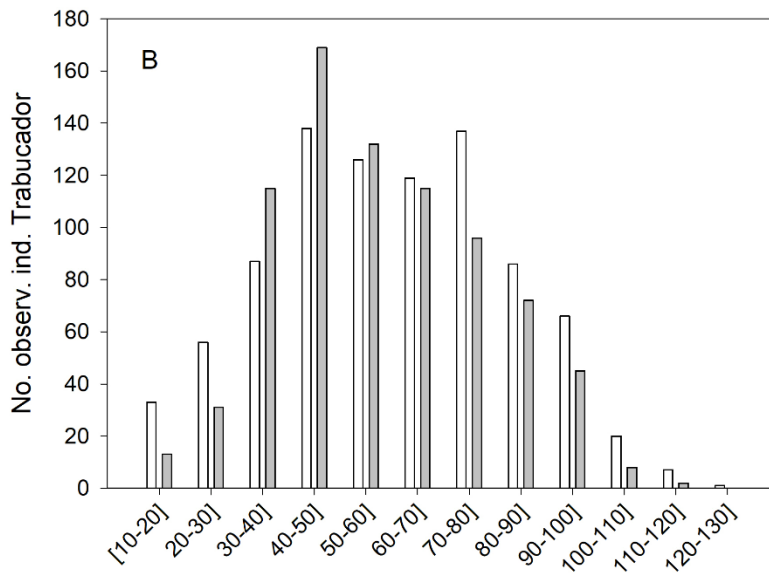
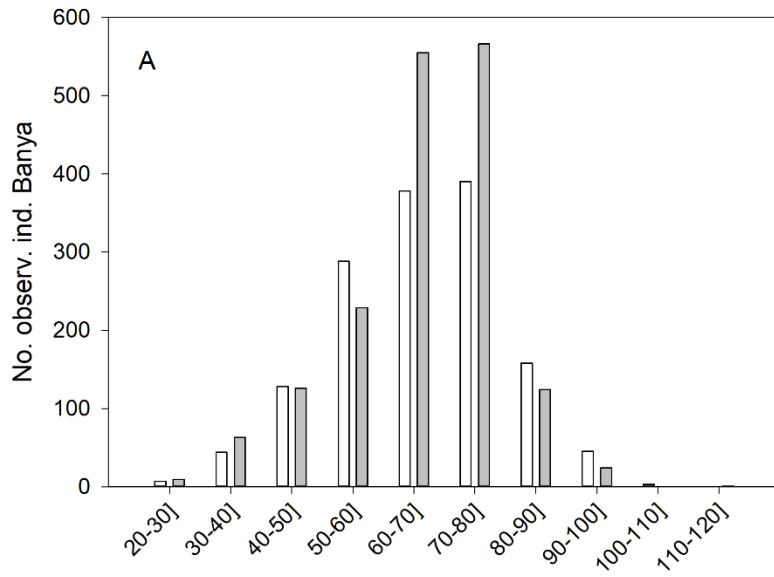
760

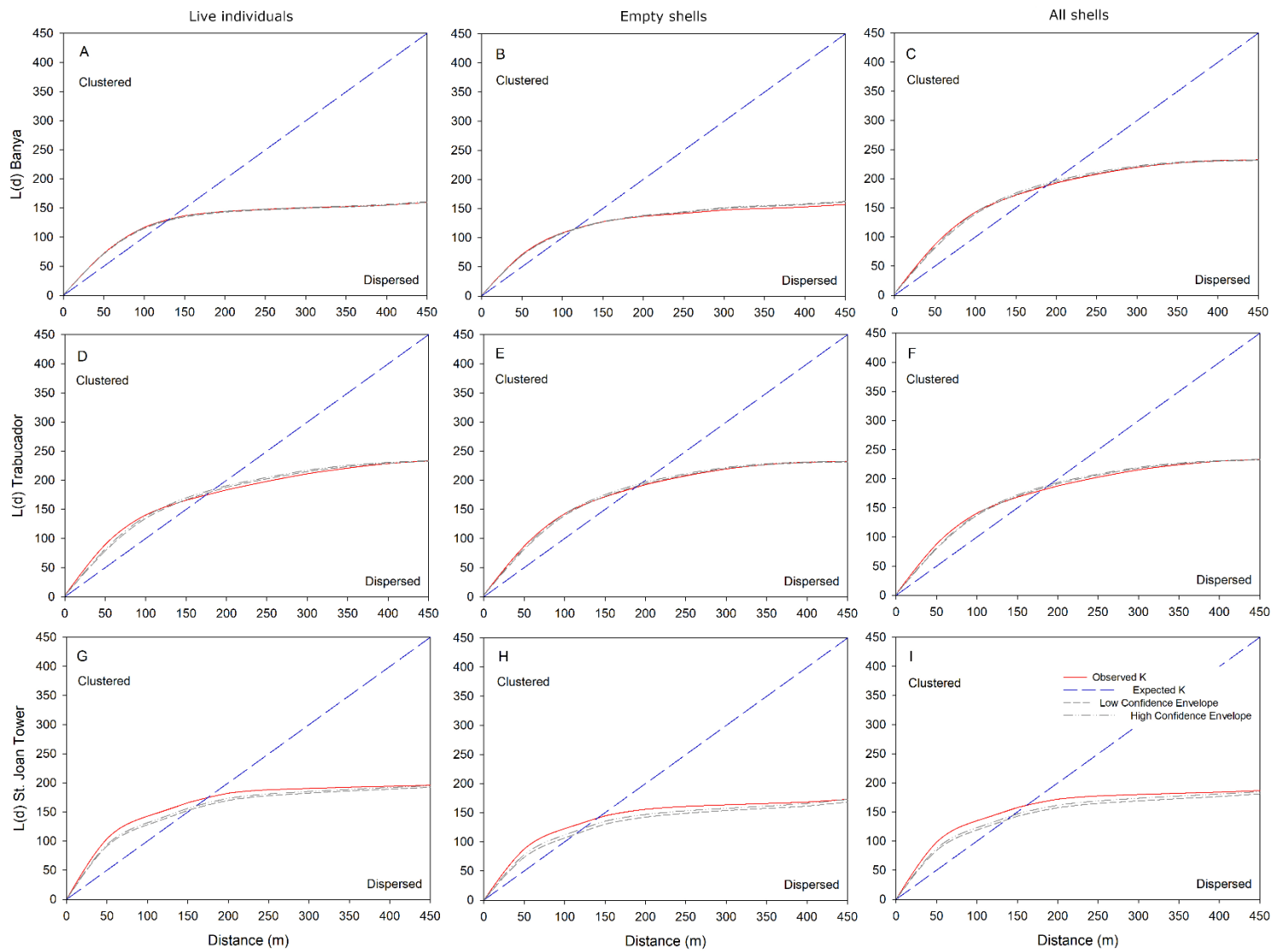
761 Fig. 2



762

763 Fig. 3





765

Fig. 5

766 **Table 1.** A-C) one-way MANOVA results showing differences among zones (Banya= B, Trabucador= T, and St. Joan Tower= ST) in the age composition  
 767 (adults= A, young adults= YA, and juveniles= J) of live individuals, empty shells, and total shells; D-F) one-way MANOVAs showing zone differences in habitat  
 768 distribution (sand= SA, Caulerpa= C, seagrass= SE, and mixed vegetation= MV) for live individuals, empty shells, and total shells; and G-I) one-way ANOVAs  
 769 for zone differences in the total abundance of live individuals, empty shells, and total shells. For each analysis, significant grouping obtained with SNK post-  
 770 hoc analyses are shown. Significant values are indicated in **bold**.  
 771  
 772

MANOVA	A) Live individuals				B) Empty Shells				C) Total shells			
<b>Age groups</b>	Wilk's $\lambda$	df	F	P	Wilk's $\lambda$	df	F	P	Wilk's $\lambda$	df	F	P
Zone	0.573	6, 272	14.50	<b>0.0000</b>	0.657	6, 272	10.57	<b>0.0000</b>	0.479	6, 272	20.11	<b>0.0000</b>
SNK (A)	B> T> ST				B> T> ST				B> T> ST			
SNK (YA)	B= T $\geq$ ST								B= T $\geq$ ST			
SNK (J)	T> B> ST								T> B> ST			
MANOVA	D) Live individuals				E) Empty Shells				F) Total shells			
<b>Habitat groups</b>	Wilk's $\lambda$	df	F	P	Wilk's $\lambda$	df	F	P	Wilk's $\lambda$	df	F	P
Zone	0.174	8, 270	46.93	<b>0.0000</b>	0.172	8, 270	47.49	<b>0.0000</b>	0.154	8, 270	52.14	<b>0.0000</b>
SNK (SA)	B> T> ST				B> T= ST				B> T> ST			
SNK (C)	ST= T> B				ST= T> B				ST= T> B			
SNK (SE)	B= T> ST				B> T> ST				B> T> ST			
SNK (MV)	T> ST= B				T> ST= B				T> ST= B			
ANOVA	G) Live individuals				H) Empty Shells				I) Total shells			
<b>Totals</b>	df	MS	F	P	df	MS	F	P	df	MS	F	P
Zone	2	4.39	21.00	<b>0.0000</b>	2	6.30	32.71	<b>0.0000</b>	2	5.74	28.75	<b>0.0000</b>
Error	138	0.21			138	0.192			138	0.199		
SNK	B> T> ST				B> T> ST				B> T> ST			

782

783 **Table 2.** Nearest Neighbor (NN) analyses for live individuals, empty shells, and all recorded  
 784 shells at each study zone. For each analysis, the nearest neighbor index, the Z-Score, the P  
 785 value, the observed mean distance (m), and the expected mean distance (m) are indicated.  
 786

	Banya center (Zone 1)			Trabucador (Zone 2)			St. Joan Tower (Zone3)		
	Live	Empty	All	Live	Empty	All	Live	Empty	All
NN Ratio	0.623	0.681	0.670	0.489	0.419	0.450	0.731	0.842	0.788
NN Z-Score	-27.32	-25.08	-35.27	-28.56	-31.38	-42.75	-10.32	-4.71	-10.31
P Value	0.000	0.000	0.000	0.000	0.000	0.000	0.000	0.000	0.000
NN Expected	2.667	2.457	1.807	4.118	4.260	2.961	5.101	6.537	4.022
NN Observed	1.663	1.675	1.212	2.014	1.786	1.333	3.732	5.510	3.171

787

788